RESEARCH ARTICLE

The *Perilla* stem aqueous extract regulation sebum synthesis in acne through the PI3K/AKT/FoxO pathway: A network pharmacology and molecular docking analysis

Mingxin Cui, Shulan Qi, Zijia Zhao, Yingxue Guo, Jiwen Cui*

College of Pharmacy, Jiamusi University, Jiamusi, Heilongjiang, China.

Received: February 23, 2024; **accepted:** April 2, 2024.

***Perilla frutescens* (L.) Britt, a member of the *Lamiaceae*, is a Chinese herbal plant renowned for its diverse pharmacological effects including anti-inflammatory, antioxidant, antibacterial, vasodilatory, hypoglycemic, and blood lipid-lowering. Notably, the *Perilla* stem aqueous extract (PSAE) holds significant promise as a novel approach in acne vulgaris (AV) treatment. Understanding the fundamental components and mechanisms through which PSAE operates in AV treatment is crucial for the development of novel therapeutic agents. This study validated PSAE's capacity to impede testosterone-induced lipid accumulation in SZ95 cells. Moreover, it delved into the pivotal components and mechanisms underlying PSAE's regulation of lipid synthesis, employing network pharmacology and molecular docking technology. The findings underscored PSAE's efficacy in effectively restraining lipid accumulation. The constituents of PSAE predominantly targeted key elements such as the androgen receptor (AR), protein kinase B (AKT), forkhead box O (FoxO), mammalian target of rapamycin (mTOR), and peroxisome proliferator activated receptor gamma (PPAR-γ), which played a crucial role in inhibiting sebaceous synthesis by modulating the phosphoinositide-3 kinase (PI3K)/AKT/FoxO pathway, consequently modulating downstream expression of mTOR and PPAR-γ. The flavonoid glycosides including luteolin-7-O-glucoside, luteolin-7-O-glucuronide, luteolin-7-O-diglucuronide, apigenin-7-O-glucuronide, and apigenin-7-O-diglucuronide, as well as organic acids like rosmarinic acid and rosmarinic acid methyl ester, and triterpenoids such as hederagenin and glochidone, demonstrated significant affinity for AKT serine/threonine kinase 1 (AKT1) and forkhead box factor 1 (FoxO1) in the PI3K/AKT/FoxO pathway. It's noteworthy that glochidone could potentially serve as a pivotal constituent within PSAE, effectively inhibiting sebaceous synthesis by targeting AKT1, FoxO1, mTOR, and PPAR-γ, showcasing robust affinity towards these targets. This study elucidated the potential of PSAE in combatting AV-related sebum synthesis *via* modulation of the PI3K/AKT/FoxO signaling pathway with glochidone emerging as a significant player component. It furnished a theoretical framework for the utilization of PSAE in anti-AV treatments.**

Keywords: *Perilla* stem; acne; network pharmacology; molecular docking; sebum synthesis.

***Corresponding author:** Jiwen Cui, School of Pharmacy, Jiamusi University, Jiamusi 154007, Heilongjiang, China. Email: cjwhljjms@163.com.

Introduction

Acne vulgaris (AV) is a prevalent, chronic inflammatory skin condition that impacts the sebaceous follicles in adolescents and adults [1]. Throughout the progression of AV, an excess of sebum secretion blocks the opening of the follicle, subsequently resulting in the formation of comedones. Bacteria subsequently proliferate within the follicles, triggering infection and

inflammatory responses, ultimately culminating in the development of AV [2]. The primary driver of AV advancement is the excessive secretion of sebum [3]. A predominant factor contributing to heightened sebum secretion among adolescent patients is the fluctuation in testosterone levels in the body [4]. When androgen binds to the androgen receptor (AR) in sebaceous cells, it activates the phosphoinositide-3 kinase (PI3K)/protein kinase B (AKT) signaling pathway. Phosphorylated AKT can then exert negative feedback on the forkhead box O (FoxO) pathway [5]. FoxO plays a critical role in regulating lipid synthesis [6], capable of inhibiting lipid synthesis by inducing the activation of the adenosine 5'-monophosphate-activated protein kinase (AMPK) pathway, thus blocking mammalian target of rapamycin (mTOR) phosphorylation and the expression of sterol regulatory element-binding protein 1 (SREBP-1) [7, 8]. Additionally, it further inhibits skin lipid synthesis by directly inhibiting the expression of PPAR-γ in the PPAR signaling pathway [9, 10].

Inhibiting sebum secretion is one of the primary approaches in current drug treatments for AV. For instance, epigallocatechin gallate (EGCG) diminishes sebum production by activating the AMPK signaling pathway, which leads to decreased expression levels of the mTOR protein and inhibition of downstream SREBP-1 expression [11, 12]. Isotretinoin, approved by the Food and Drug Administration (FDA) as an effective treatment for severe refractory AV [13], can curb excessive sebum production by upregulating the expression of nuclear forkhead box factor 1 (FoxO1) protein [14]. Given the challenge of completely eradicating AV and its propensity for recurrence, prolonged use of chemical medications can foster drug resistance and trigger assorted side effects, including dryness, erythema, and stinging sensations, and in severe cases, may even induce teratogenic effects [15]. Hence, the imperative to innovate and develop new therapeutic drugs for AV treatment remains paramount. Plant extracts present a promising avenue for AV treatment due to their multi-component, multi-target therapeutic approach, and minimal side effects [16, 17]. However, elucidating the crucial components and underlying mechanisms of action is essential in the medication development process. Network pharmacology emerges as a valuable tool for deciphering the intricate interactions among components, targets, and diseases [18], facilitating the identification of pivotal components and therapeutic targets within complex plant extracts. Additionally, molecular docking methods prove instrumental in elucidating the binding affinity and mode of action between each component and its target site [19–21].

Perilla frutescens (L.) Britt, a widely known herbaceous plant, manifests diverse therapeutic effects across its leaves, seeds, and stems [22, 23]. Particularly noteworthy is *Perilla frutescens* seed oil, abundant in essential fatty acids crucial for human health, thus holding significant nutritional and commercial value [24]. *Perilla frutescens* cultivation on a large scale presents significant economic benefits [25]. Nevertheless, post-harvesting, a substantial amount of *Perilla* stems is often left unused, typically deemed as waste. Commonly employed methods for managing this waste include incineration and landfilling, which not only contributes to environmental pollution but also results in the wastage of numerous naturally occurring active ingredients. Conducting comprehensive research on the pharmacological effects and active constituents of *Perilla* stems is imperative to augment their practical value. It had been discovered that the alcohol extract from *Perilla* could decrease the activity of the fat-producing gene PPAR-γ and increased the expression of lipolytic genes at the mRNA level. Consequently, it reduced the quantity of triglycerides in 3T3-L1 cells and diminished adipocyte lipid accumulation [26]. Furthermore, luteolin in the alcohol extract from *Perilla* has been demonstrated to possess anti-inflammatory properties, capable of reducing inflammatory cytokines such as tumor necrosis factor alpha (TNF-α), interleukin-6 (IL-6), and interleukin-8 (IL-8) expression [27–29]. These studies have

demonstrated the anti-inflammatory and blood lipid-lowering effects of *Perilla* extracts. However, research on water extracts has been relatively scarce with the majority of studies focusing on alcohol extracts from *Perilla*. Specifically, the mechanism of anti-AV activity of complex components in aqueous extract remains unclear. Compared to alcohol extracts, water extracts are more readily compatible in application and development processes, which may confer an advantage. In this study, the human sebaceous (SZ95) cells were employed as a model, and lipid secretion was stimulated by testosterone (T) to assess the inhibitory effect of PSAE on lipid accumulation. The study employed network pharmacology to ascertain the fundamental components and specific pathways through which PSAE regulates lipid synthesis, aiming to clarify the mode of action of key PSAE components. Molecular docking technology was utilized to further elucidate the binding affinity and mechanism of action between each component and its target site. The findings of this study would offer a theoretical framework for the application of *Perilla* stem in the field of anti-AV treatment, warranting further experimental verification.

Materials and methods

Preparation of *Perilla* stem water extract

The stems of *Perilla frutescens* were collected from Jiamusi, Heilongjiang, China in July 2022. 100 g *Perilla* stems were placed in a 3,000 mL round-bottom flask with addition of 2,500 mL of distilled water to achieve a solid-liquid ratio of 1:25. The *Perilla* stems were soaked in water overnight, then subjected to a 1-hour reflux extraction, and the extract was filtered. An equal amount of distilled water was added to the residue followed by continued reflux extraction for 1 hour, and the extract was filtered again. The same step was repeated three times. The three filtered extracts were mixed and dried to powder for further experiments.

Cell culture, treatment, and MTT assay

SZ95 cells were purchased from Biobw, Beijing, China and cultured in DMEM (BOSTER, Wuhan, Hubei, China) supplemented with 10% Fetal bovine serum (FBS) and 1% penicillin/streptomycin (Beyotime, Shanghai, China) at 37°C in a 5% CO_2 incubator (Thermo Fisher Scientific, Waltham, MA, USA). SZ95 cells in the logarithmic growth phase were collected, trypsinized, and centrifuged. The cell suspension was adjusted to a concentration of 3×10^4 cells/mL using complete medium, and 200 µL of the suspension was added to each well in 96-well plates. After 24 hours of cultivation, the cell samples were exposed to various concentrations of *Perilla* stem extract (PSAE) at 0, 1,000, 1,500, 2,000, 2,500, and 3,000 µg/mL, as well as different concentrations of isotretinoin (Macklin, Shanghai, China) and testosterone (T) (Solarbio, Beijing, China) at 0, 5, 10, 20, 40, and 80 µg/mL. Each group was replicated in 3 wells. After incubating for 24 h, 20 µL of 5 mg/mL Methylthiazolyldiphenyl-tetrazolium bromide (MTT) (Beyotime, Shanghai, China) solution was added to each well in the dark, and the culture was continued for 4 h. The medium was then removed, and 150 µL of Dimethyl sulfoxide (DMSO) (Biotopped, Beijing, China) was added to each well. The absorbance of each well was measured at 490 nm using a microplate reader (Thermo Fisher Scientific, Waltham, MA, USA) to calculate the cell viability. The cells were shaken for 10 min before measurement to ensure complete dissolution of the formazan crystals within the cells.

$$\text{Cell viability \%} = \frac{A_{exp} - A_{blank}}{A_{Control} - A_{blank}} \times 100\% \quad (1)$$

where A_{exp} and $A_{Control}$ were the absorbency of cells in the drug group and the blank control group, respectively. A_{blank} was the absorbency of blank medium without cells.

Triglyceride (TG) quantification and Nile red staining

After removing the medicated medium, the cells were washed twice with phosphate buffered saline (PBS) (BOSTER, Wuhan, Hubei, China).

After trypsin digestion, the cells were centrifuged at 1,000 rpm for 10 min. Subsequently, the cells were lysed with 200 µL of 2% Triton X-100 (Macklin, Shanghai, China) for 40 min and then detected using a Triglyceride (TG) kit (Nanjing Jiancheng Bioengineering Institute, Nanjing, Jiangsu, China) following manufacturer's instructions. After discarding the medicated medium, the cell sample was washed twice with PBS and then fixed in 4% paraformaldehyde (Beyotime, Shanghai, China) for 10 min at room temperature before Nile red staining. After fixation, 100 µg/mL Nile red (Macklin, Shanghai, China) staining solution was added and incubated in an incubator at 37°C for 10 min. The staining solution was removed and washed with PBS 3 to 5 times. The DAPI staining solution was added and kept in the dark at room temperature for 20 min. After washing with PBS for 3 to 5 times, the cells were gently removed and placed on the slide, and 10 µL of anti-fluorescence quenching sealing agent (BOSTER, Wuhan, Hubei, China) was added drop by drop. The staining was observed using Leica DMI4000 B fluorescence microscope (Leica, Wetzlar, Germany). The cells exhibiting strong orange-red fluorescence were positively identified as lipid-rich cells.

Collecting bioactive compounds and gene targets of PSAE

The chemical information of the potential active compounds in PSAE such as canonical SMILES, molecular formula, molecular weight, structure, and PubChem ID was gathered by using PubChem (https://pubchem.ncbi.nlm.nih.gov/). Then the canonical SMILES of these active compounds was imported into SwissTargetPrediction (http://www.swisstargetprediction.ch/) to identify their therapeutic targets. The obtained target genes were combined and checked for duplicates to identify potential targets for treating diseases using the PSAE.

Collection of repetitive targets related to PSAE and sebum

The keywords "Sebum synthesis and metabolism" and "Lipogenesis" were utilized to retrieve targets from Online Mendelian Inheritance in Man (OMIM) (https://omim.org/) and GeneCards (https://www.genecards.org). Subsequently, the targets were combined, and any duplicates were removed to create a list of targets for sebum-related diseases. The overlap between the target genes of PSAE and sebum-associated genes was illustrated using a Venn diagram (https://bioinfogp.cnb.csic.es/tools/venny/).

Active ingredients-target network establishment

Cytoscape 3.10.1 (https://cytoscape.org/) was utilized to construct the "active ingredients-target" network. In this network, active ingredients and targets were depicted as distinct graphical nodes with interconnections between them represented by edges.

PPI network construction

The intersection of genes between PSAE and sebum was imported into the STRING database (https://www.string-db.org/) with the species limited to "Homo sapiens" and confidence data set at > 0.7 to construct the PPI network. A visual network analysis was plotted by using Cytoscape 3.10.1. Core targets with a degree greater than 10 and related to sebum synthesis were obtained from Centiscape analysis.

Gene Ontology (GO) function and KEGG pathway enrichment analyses

The DAVID (Database for Annotation, Visualization, and Integrated Discovery) database (http://david.abcc.ncifcrf.gov/), accessed on December 31, 2023, is an online, free bioinformatics database used for analyzing differential gene function and pathway enrichment. Potential targets obtained from Gene Ontology Function Annotation (GO) were analyzed online and imported into DAVID, which included the potential targets and their associated signaling pathways (KEGG). The analysis results were then visualized by creating bubble plots using the bioinformatics database (https://www.bioinformatics.com.cn/).

Molecular docking

The PubChem database was accessed on December 31, 2023 to download the 3D structures of 17 compounds including luteolin-7-O-glucoside, luteolin-7-O-glucuronide, luteolin 7-O-diglucuronide, apigenin-7-glucuronide, apigenin-7-O-diglucuronide, caffeic acid, methyl caffeate, ethyl caffeate, rosmarinic acid, rosmarinic acid methyl ester, salvianic acid A, hederagenin, glochidone, 6,7-dihydroxycoumarin, tyrosine, adenosine, and phenylalanine. The PDB database (https://www.rcsb.org/) was used to download the structure of the receptor proteins AR (1t7t), AKT1 (6hhg), FoxO1 (4lg0), mTOR (1fap), and PPAR-γ (3adx). The water of crystallization and other inactive ligands were removed from the receptor protein structure using PyMOL software (Version 2.5.2) (https://pymol.org/). Hydrogen atoms had been added and preserved. In this study, the AutoDockTool (1.5.6) (https://autodocksuite.scripps.edu/adt/) was utilized. The software was hydrogenated and charged, and the AutoDock Vina 1.5.6 software was employed for molecular docking. Since the docking box size contains the binding site for the protein, the molecular docking result was selected as the best conformation for docking, and it was visualized using PyMOL. Further, the binding energy scores were extracted and ranked.

Statistical analyses

SPSS version 29 (IBM, Armonk, New York, USA) was employed for data statistical analysis. Data were measured at least three times and expressed as mean ± standard deviation. Statistical differences were assessed using analysis of variance (ANOVA). Statistical significance was set at $P < 0.05$, $P < 0.01$, and $P < 0.001$ as significant, very significant, and extremely significant, respectively.

Results and discussion

Effects of PSAE on lipid accumulation in SZ95 cells

The results of the effects of testosterone (T), isotretinoin, and PSAE on the viability of SZ95 cells showed that, up to 2,000 μg/mL of PSAE, the cell viability was still greater than 91.69%. However, as the PSAE concentration rose, the viability of SZ95 cells sharply decreased ($P < 0.05$) (Figure 1A). Therefore, dosages of 2,000, 1,000, and 500 μg/mL were used to define the high, medium, and low dose groups, respectively. Over 90.56% of the cells were still viable at 10 μg/mL of T and 90.66% at 40 μg/mL of sotretinoin (Figure 1B). Therefore, 10 μg/mL of T and 40 μg/mL of sotretinoin were selected for additional study. Triglyceride (TG) is the primary component of skin lipids and is commonly used as an indicator to detect changes in lipid content [15, 30]. In adolescent patients, T plays a key role in regulating skin oil secretion [31]. The inhibitory effect of PSAE on T-induced TG accumulation in SZ95 cells was showed in Figure 1C. After treatment with T, the TG content of SZ95 cells increased by 2.5 times compared to the control group ($P < 0.001$). The cells treated with isotretinoin significantly reduced the TG content of T-induced SZ95 cells, bringing the intracellular TG level close to that of the control group ($P > 0.05$). The PSAE treatment group also significantly reduced the TG content of T-induced SZ95 cells in a dose-dependent manner. The intracellular T-induced TG content in the high-dose PSAE group did not show a significant difference from that in the control group ($P > 0.05$), indicating an inhibitory effect similar to that of isotretinoin within the safe dose range. Nile red, a lipid-soluble fluorescent marker, exhibits intense orange-red fluorescence at a 530 nm excitation wavelength upon binding to lipids, and is often used to determine cell lipid content [17]. In the study, SZ95 cells were stained with Nile red to assess their intracellular lipid levels. The fluorescence intensity was analyzed using Image J software (Figures 1D and 1E). The results revealed that the fluorescence intensity of SZ95 cells was significantly enhanced after T treatment by 2.3 times compared to the control group ($P < 0.001$). However, when cells were co-treated with isotretinoin and T, the fluorescence intensity caused by T was significantly reduced.

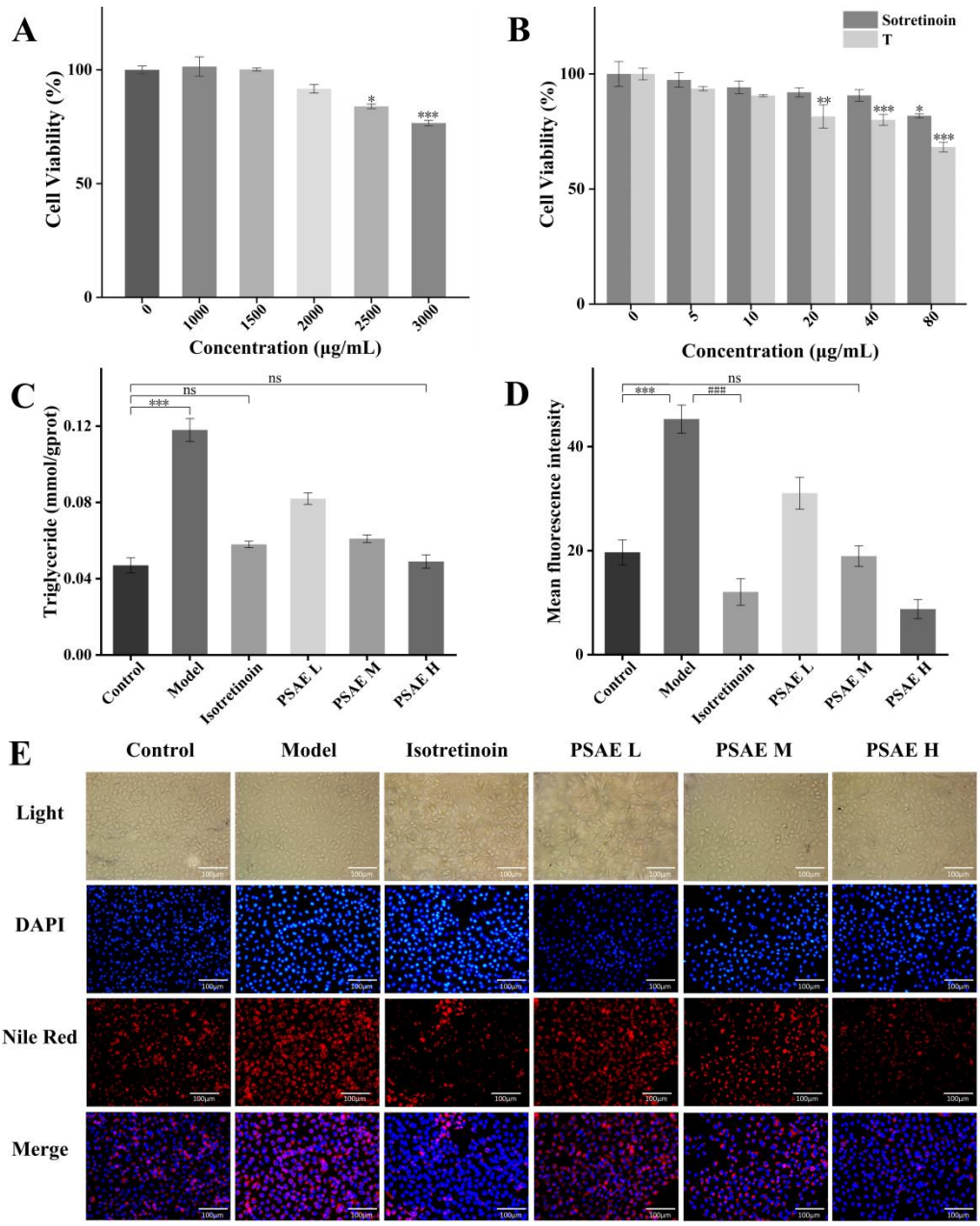

Figure 1. Cell viability of SZ95 cells exposed to the *Perilla* stem aqueous extract (A) and testosterone and isotretinoin (B). Triglyceride content (C). Quantitative analysis of fluorescence following Nile Red staining (D). The photofluorogram of Nile Red and DAPI staining of *Perilla* stem aqueous extract, testosterone, and isotretinoin with scale bar of 100 μm (E). The data are presented as the mean ± standard deviation (n=3). $^{*}P < 0.05$, $^{**}P < 0.01$, $^{***}P < 0.001$ were the comparison with the control group. $^{###}P < 0.001$ was the comparison with the model group.

Compared to the model group, the fluorescence intensity decreased by 3.7 times ($P < 0.001$), significantly lower than that of the control group. As the PSAE dosage increased, the fluorescence intensity of the cells gradually decreased. The fluorescence intensity of cells in the medium dose group of PSAE was similar to that of the control group ($P > 0.05$). However, the fluorescence intensity of cells exposed to the high dose group of PSAE was significantly lower than that of the control group, and even lower than that of the isotretinoin group. The results indicated that PSAE had a strong inhibitory effect on lipid secretion. Within the safe dosage range,

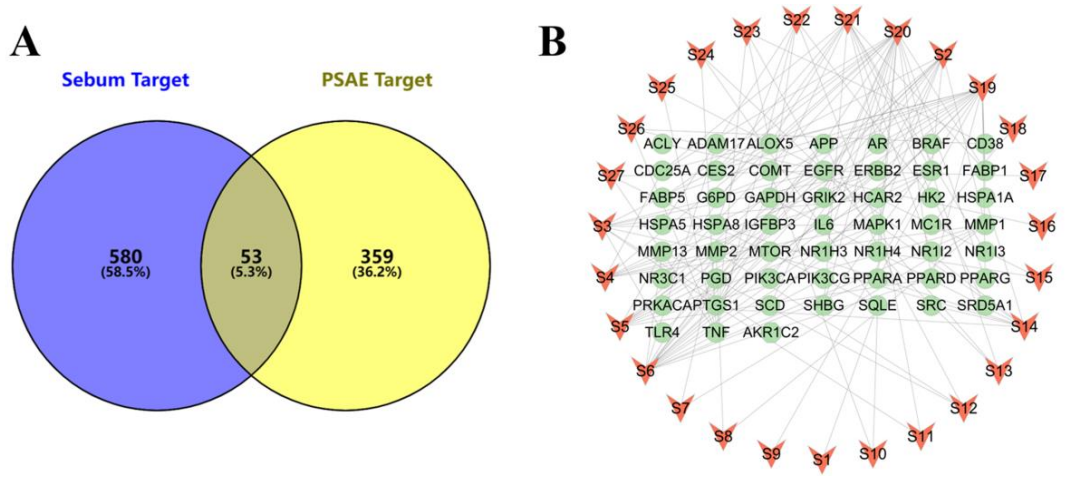

Figure 2. Network pharmacology analysis of the *Perilla* stem aqueous extract for treating skin lipid accumulation. (A) The intersection of target genes in PSAE and sebum. (B) Drug component-target network. The red polygon node represented the active ingredient of *perilla* stem decoction, while the green hexagon node represented the disease gene.

the inhibitory effect of PSAE for lipid secretion was even better than that of isotretinoin.

Collection of active components of PSAE

Twenty-seven (27) active compounds in PSAE were collected according to the previous reported methods [32–37], primarily including flavonoid glycosides, phenolic acids, triterpenoids, and coumarins, as well as a small amount of fatty acids and amino acids (Supplementary Table 1). The flavonoid glycoside components included luteolin-7-O-glucoside, luteolin-7-O-glucuronide, luteolin-7-O-diglucuronide, apigenin-7-glucuronide, and apigenin-7-O-diglucuronide. The phenolic acid components included gallic acid, caffeic acid, methyl caffeate, ethyl caffeate, rosmarinic acid, methyl rosmarinate, 3,3'-ethoxy rosmarinic acid, catechin, salvianic acid A, protocatechuic acid, chlorogenic acid, citric acid, and hydrocinnamic acid. The triterpenoid components included hederagenin and glochidone. The fatty acid component included jasmonic acid, and the coumarin component included 6,7-dihydroxycoumarin. The amino acid components included tyrosine, adenosine, pyroglutamic acid, phenylalanine, and tryptophan. The canonical SMILES, chemical formulas, molecular weights, and PubChem IDs for 27 compounds were downloaded from PubChem. The potential targets of each compound were predicted using the SwissTargetPrediction platform. All targets were combined, and duplicates were removed, resulting in a total of 412 targets.

Target prediction

The keywords of "sebum synthesis and metabolism" and "lipogenesis" gene targets were collected from the OMIM and GeneCards databases, and after removing the same targets, 633 gene targets were obtained as therapeutic targets related to sebum. The Venn diagram revealed that a total of 53 common targets were identified through matching 412 drug targets and 633 disease targets (Figure 2A). These 53 common targets were potential candidates for PSAE in the treatment of sebum-related diseases. The "active ingredient-therapeutic target" network was constructed using Cytoscape 3.10.1 to further identify the key molecular mechanisms involving 27 ingredients and 53 potential targets. This network comprised 80 nodes and 154 edges, and all 27 ingredients could interact with multiple genes associated with sebaceous synthesis and metabolism (Figure 2B). The results indicated that PSAE and its ingredients might affect multiple targets, leading to complex pharmacological changes and comprehensive overall effects.

Table 1. Topology analysis of core targets in the PPI network.

Gene	Degree	Betweenness centrality	Closeness centrality
PPARG	30	0.114657874	0.725806452
MTOR	19	0.020436749	0.608108108
PPARA	19	0.04409432	0.625
AR	15	0.034970284	0.584415584
PPARD	14	0.012526136	0.5625

Protein-protein interaction (PPI) construction and analysis

In order to explore the mechanism by which the active ingredients in PSAE reduced the production of sebum, a protein-protein interaction (PPI) network was constructed by entering the 53 targets into the STRING database. The PPI network was then topologically analyzed using Cytoscape 3.10.1. PPAR-γ, mTOR, PPAR-α, AR, and PPAR-δ were identified as important targets that regulated lipid synthesis with a degree larger than 10 (Table 1). PPAR-γ, PPAR-α, and PPAR-δ are three subtypes of the PPAR receptor. PPAR-γ is mostly expressed in sebocytes and regulates the lipid-generating pathway in sebocytes [38]. As a result, it was thought to be a suitable target for controlling lipid production [9, 39]. The lipid kinase domain of the mTOR complex regulates fat synthesis *via* the mTOR pathway, which controls the expression of SREBP1 that affects fatty acid production [40]. Nuclear receptor AR binds to either dihydrotestosterone (DHT) or testosterone (T) in the cytoplasm. Following its transfer to the nucleus, the protein gets activated, which raises the synthesis of lipids [41, 42]. According to PPI information, the ingredient of PSAE might control lipid synthesis in SZ95 cells by influencing PPAR-γ, mTOR, and AR, three important targets.

Gene Ontology and KEGG pathway enrichment

To identify the metabolic pathways and biological processes that PSAE might inhibit sebum production, KEGG enrichment and Gene Ontology (GO) functional annotation analyses were performed on 53 intersecting genes. Biological processes (BP), cellular components (CC), and molecular functions (MF) were all included in the GO analysis. The major biological functions associated with gene products were referred to as biological processes (BP). The cellular component in which gene products function was referred to as the CC. The molecular functions performed by gene products was referred to as MF [43]. According to the BP analysis, these targets primarily impacted gene expression, exerted negative control over the process of apoptosis, and modulated intracellular receptor signaling pathways. Based on the CC analysis, 53 cross-targets were primarily involved in the cytoplasm and perinuclear cytoplasm. According to the MF analysis, these targets mostly affected sequence-specific DNA binding, RNA polymerase II transcription factor activity, and the binding of homologous proteins (Figure 3A). Among the three main targets identified by the PPI analysis, mTOR controlled protein binding, while PPAR-γ and AR controlled RNA polymerase II transcription factor activity and sequence-specific DNA binding. KEGG pathway enrichment analysis found that the 53 crossing targets were largely enriched in the PPAR, PI3K/AKT, FoxO, and mTOR signaling pathways, all of which were linked to skin lipid secretion (Figure 3B). The PI3K/AKT pathway is activated by AR activation, and by activating AKT protein kinase, the PI3K enzyme suppresses the activity of the downstream FoxO transcription factor. The PI3K/AKT/FoxO pathway regulates sebaceous gland lipid secretion by activating downstream mTOR and PPAR signaling pathways, which enhances lipid synthesis (Figure 3C).

Identification of key components that inhibit sebum synthesis in PSAE

PSAE regulated skin lipid synthesis by modulating the expression of AR, the PI3K/AKT/FoxO

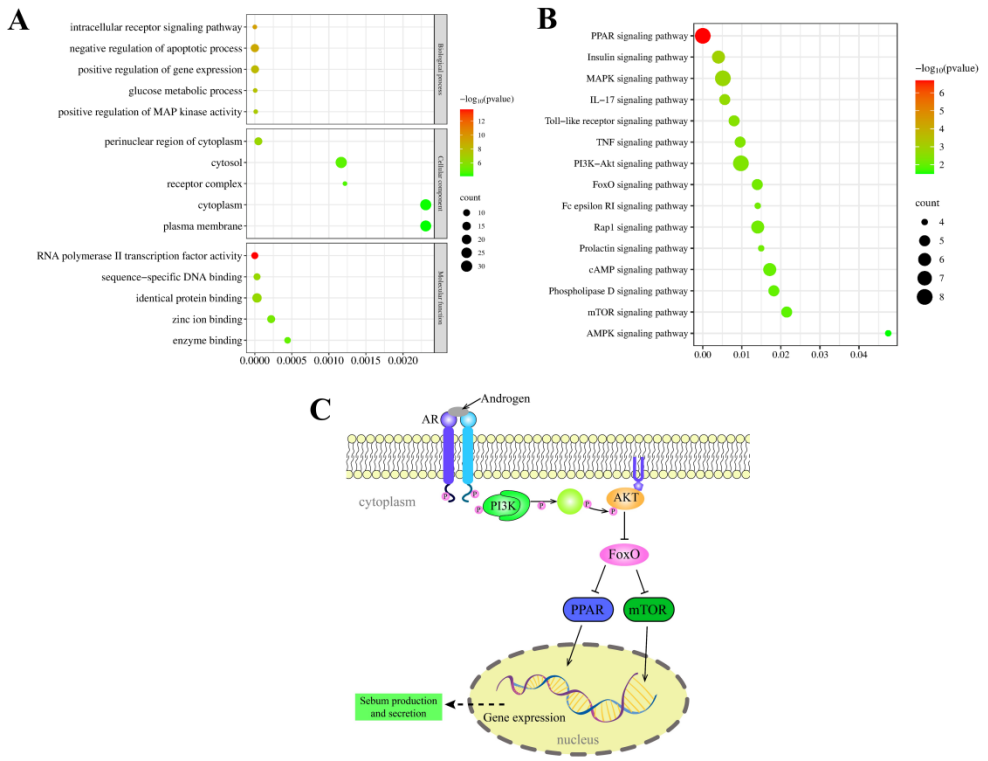

Figure 3. The analysis of GO enrichment (A), KEGG pathway enrichment (B), and the chart of PI3K-AKT, FoxO, mTOR, and PPAR signaling pathways (C).

signaling pathway, mTOR, and PPAR-γ. The overexpression of AR caused by excessive secretion of androgen is the primary factor that induces sebum synthesis. PSAE might contain 3 out of 27 active ingredients associated with AR (Figure 4), including hederagenin, glochidone, and jasmonic acid. In addition, 17 components, including flavonoid glycosides such as luteolin-7-O-glucoside, luteolin-7-O-glucuronide, luteolin 7-O-diglucuronide, apigenin-7-glucuronide, and apigenin-7-O-diglucuronide, organic acid components such as caffeic acid, methyl caffeate, ethyl caffeate, rosmarinic acid, rosmarinic acid methyl ester, and salvianic acid A, triterpenoid components such as hederagenin and glochidone, coumarin compound 6,7-dihydroxycoumarin, and amino acid substances such as tyrosine, adenosine, and phenylalanine, regulated the PI3K/AKT/FoxO signaling pathway, and might play a role in inhibiting sebum secretion (Figure 4). It is worth noting that glochidone can simultaneously regulate the expression of AR, the PI3K/AKT/FoxO signaling pathway, mTOR, and PPAR-γ. It may play a crucial role in the lipid synthesis process regulated by PSAE.

Visualization of molecular docking results analysis

A Molecular docking test was conducted using Auto dock 1.5.6 to assess the binding affinity of each component with the target proteins. The binding energy (kcal/mol) was determined through docking analysis. A lower score indicated a stronger binding ability. When the binding energy was less than -5 kcal/mol, the binding condition was considered favorable, and when it was less than -7 kcal/mol, the binding condition was considered strong [44]. Docking results revealed that hederagenin and jasmonic acid exhibited strong binding affinities to AR with binding energies of -8.2 and -7.1 kcal/mol, respectively (Table 2) (Supplementary Table 2). The two components might be crucial for

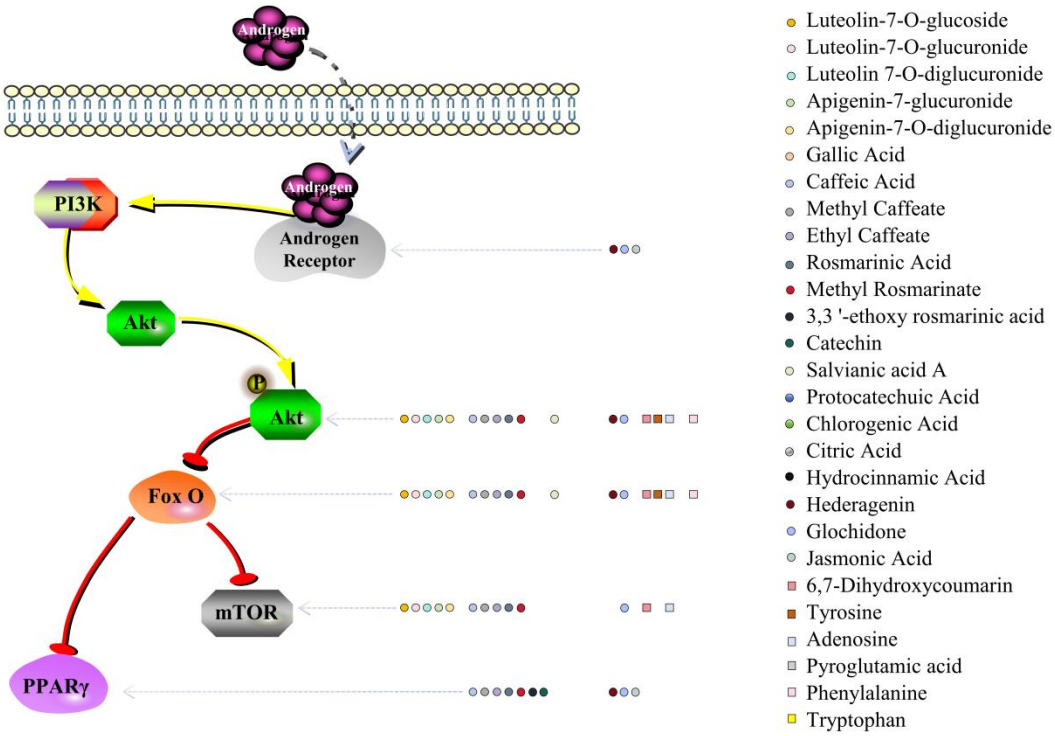

Figure 4. Identification of key components inhibiting sebum synthesis in PSAE.

Table 2. Molecular docking binding energy (kcal/mol).

	AR	AKT1	FoxO1	mTOR	PPAR-γ
Luteolin-7-O-glucoside	-	-10.9	-8.3-	-	-
Luteolin-7-O-glucuronide	-	-11.3	-8.8	-	-
Luteolin 7-O-diglucuronide	-	-11.9	-8.6	-	-
Apigenin-7-glucuronide	-	-11.3	-8.7	-	-
Apigenin-7-O-diglucuronide	-	-11.1	-8.8	-	-
Caffeic Acid	-	-6.7	-6.9	-	-
Methyl Caffeate	-	-6.7	-6.8	-	-
Ethyl Caffeate	-	-7.0	-6.8	-	-
Rosmarinic Acid	-	-9.1	-7.6	-	-
Methyl Rosmarinate	-	-8.6	-7.2	-	-
Salvianic acid A	-	-6.7	-7.0	-	-
Hederagenin	-8.2	-10.5	-7.9	-	-
Glochidone	-1.8	-8.5	-8.0	-8.6	-7.9
Jasmonic Acid	-7.1	-	-	-	-
6,7-Dihydroxycoumarin	-	-7.0	-6.5	-	-
Tyrosine	-	-6.3	-6.5	-	-
Adenosine	-	-7.1	-6.7	-	-
Phenylalanine	-	-6.6	-6.5	-	-

inhibiting AR expression in PSAE. The docking results of 17 components targeting the PI3K/AKT/FoxO pathway with AKT1 and FoxO1 indicated that the flavonoid glycosides including

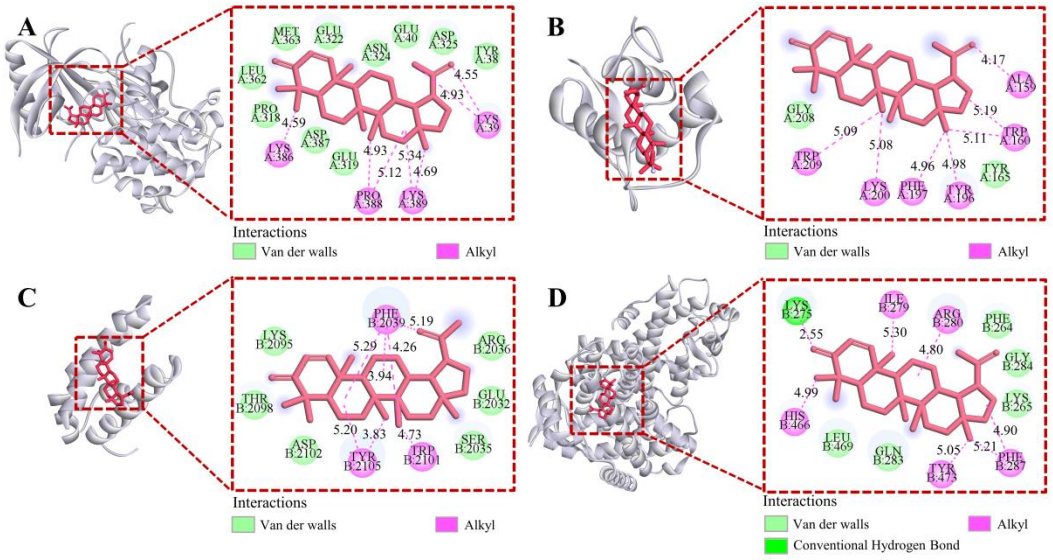

Figure 5. Molecular docking diagrams with 2D and 3D plots. (A) Glochidone - AKT1. (B) Glochidone - FoxO1. (C) Glochidone – mTOR. (D) Glochidone – PPAR-γ complexes. AR: androgen receptor. AKT: serine/threonine protein kinase. FoxO1: forkhead box O1. mTOR: mammalian target of rapamycin. PPAR-γ: peroxisome proliferator-activated receptor γ.

luteolin-7-O-glucoside, luteolin-7-O-glucuronide, luteolin 7-O-diglucuronide, apigenin-7-glucuronide, and apigenin-7-O-diglucuronide exhibited the highest binding energies to AKT1 with the values of -10.9, -11.3, -11.9, -11.3, and -11.1 kcal/mol, respectively. The organic acid components, rosmarinic acid and rosmarinic acid methyl ester, and the triterpenoid components, hederagenin and glochidone, also showed high affinities for the core protein AKT1 with binding energies of -9.1, -8.6, -10.5, and -8.5 kcal/mol, respectively (Table 2) (Supplementary Table 3). These nine components also exhibited strong affinities for FoxO1 with binding energies of -8.3, -8.8, -8.6, -8.7, -8.8, -7.6, -7.2, -7.9, and -8.0 kcal/mol, respectively, and might play important roles in inhibiting sebaceous synthesis (Table 2) (Supplementary Table 4). The molecular docking results of glochidone with AR, AKT1, FoxO1, mTOR, and PPAR-γ showed that glochidone had strong binding abilities to four proteins including AKT1, FoxO1, mTOR, and PPAR-γ with binding energies of -8.5, -8.0, -8.6, and -7.9 kcal/mol, respectively (Table 2) (Supplementary Table 5). Although glochidone had a weaker binding ability to AR, it exhibited strong binding abilities to the four proteins related to the pathway. These proteins might be key targets in the regulation of lipid synthesis by PSAE. The molecular docking visualization analysis indicated that the residues Lys39, Pro388, Lys386, and Lys389 in the AKT1 protein, as well as Trp209, Phe197, Tyr196, Trp160, Ala159, and Lys200 in the FoxO1 protein, and Tyr2105, Phe2039, Tyr2105, and Trp2101 in the mTOR protein formed hydrophobic bonds with glochidone (Figure 5). These residues were in the active sites of the respective proteins. Additionally, the residues Lys275, Arg280, Ile279, Phe287, Tyr473, and His466 in the PPAR-γ protein formed hydrophobic and hydrogen bonds with glochidone. These results indicated that glochidone exerted its biological activity by interacting with specific amino acid residues in the active sites of these proteins.

Conclusion

PSAE demonstrated promising potential as an effective inhibitor of sebum synthesis, suggesting its viability as a potent anti-AV medication. Network pharmacology and molecular docking studies indicated that the 5 kinds of flavonoid glycosides, 2 kinds of organic acids, and 2 kinds of

triterpenoids in PSAE exerted significant inhibitory effects on sebum synthesis by regulating the PI3K/AKT/FoxO pathway. Particularly noteworthy was the impact of glochidone on AKT1, FoxO1, mTOR, and PPAR-γ, showcasing strong affinity toward these downstream targets, which underscored the potential of glochidone as a key component driving the efficacy of PSAE. This study employed bioinformatics methodologies to preliminarily investigate and predict the mechanism underlying PSAE's anti-sebum synthesis effects, laying a foundational framework for further experimental inquiries into drug development.

Acknowledgement

This research was supported by the Heilongjiang Province Key Research and Development Plan Project (Grant No. JD22A016), Heilongjiang Province "Double first-class" Discipline Collaborative Innovation Achievement Construction Project (Grant No. LJGXCG2023-041), Basic Scientific Research Project for Heilongjiang Provincial Colleges and Universities (Grant No. 2021-KYYWF-0590), and Heilongjiang Huahao Testing Technology Service Co., LTD.

References

1. Wu J, Guo R, Chai J, Xiong W, Tian M, Lu W, *et al*. 2021. The protective effects of Cath-MH with anti-*Propionibacterium* acnes and anti-inflammation functions on acne vulgaris. Front Pharmacol. 12:788358.
2. De Canha MN, Komarnytsky S, Langhansova L, Lall N. 2020. Exploring the anti-acne potential of *Impepho* [*Helichrysum odoratissimum* (L.) Sweet] to combat *Cutibacterium* acnes virulence. Front Pharmacol. 10:1559.
3. Zouboulis CC, Jourdan E, Picardo M. 2014. Acne is an inflammatory disease and alterations of sebum composition initiate acne lesions. J Eur Acad Dermatol. 28(5):527-532.
4. Yin J, Hwang IH, Lee MW. 2019. Anti-acne vulgaris effect including skin barrier improvement and 5α-reductase inhibition by tellimagrandin I from *Carpinus tschonoskii*. BMC Complem Altern M. 19(1):323.
5. Lai JJ, Chang P, Lai KP, Chen L, Chang C. 2012. The role of androgen and androgen receptor in skin-related disorders. Arch Dermatol Res. 304(7):499-510.
6. Li Y, Ma Z, Jiang S, Hu W, Li T, Di S, *et al*. 2017. A global perspective on FOXO1 in lipid metabolism and lipid-related diseases. Prog Lipid Res. 66:42-49.
7. Agamia NF, Abdallah DM, Sorour O, Mourad B, Younan DN. 2016. Skin expression of mammalian target of rapamycin and forkhead box transcription factor O1, and serum insulin-like growth factor-1 in patients with acne vulgaris and their relationship with diet. Brit J Dermatol. 174(6):1299-1307.
8. Monfrecola G, Lembo S, Caiazzo G, De Vita V, Di Caprio R, Balato A, *et al*. 2016. Mechanistic target of rapamycin (mTOR) expression is increased in acne patients' skin. Exp Dermatol. 25(2):153-155.
9. Mastrofrancesco A, Ottaviani M, Cardinali G, Flori E, Briganti S, Ludovici M, *et al*. 2017. Pharmacological PPAR-γ modulation regulates sebogenesis and inflammation in SZ95 human sebocytes. Biochem Pharmacol. 138:96-106.
10. Coenye T, Peeters E, Nelis HJ. 2007. Biofilm formation by *Propionibacterium* acnes is associated with increased resistance to antimicrobial agents and increased production of putative virulence factors. Res Microbiol. 158(4):386-392.
11. Im M, Kim SY, Sohn KC, Choi DK, Lee Y, Seo YJ, *et al*. 2012. Epigallocatechin-3-gallate suppresses IGF-I-induced lipogenesis and cytokine expression in SZ95 sebocytes. J Invest Dermatol. 132(12):2700-2708.
12. Yoon JY, Kwon HH, Min SU, Thiboutot DM, Suh DH. 2013. Epigallocatechin-3-gallate improves acne in humans by modulating intracellular molecular targets and inhibiting P. acnes. J Invest Dermatol. 133(2):429-440.
13. Zaenglein AL, Pathy AL, Schlosser BJ, Alikhan A, Baldwin HE, Berson DS, *et al*. 2016. Guidelines of care for the management of acne vulgaris. J Am Acad Dermatol. 74(5):945-973.
14. Agamia NF, Hussein OM, Abdelmaksoud RES, Abdalla DM, Talaat IM, Zaki EI, *et al*. 2018. Effect of oral isotretinoin on the nucleo-cytoplasmic distribution of FoxO1 and FoxO3 proteins in sebaceous glands of patients with acne vulgaris. Exp DermatoL. 27(12):1344-1351.
15. Jin S, Lee MY. 2018. Kaempferia parviflora extract as a potential anti-acne agent with anti-inflammatory, sebostatic and anti-propionibacterium acnes activity. Int J Mol Sci. 19(11):3457.
16. Wu J, Pan L. 2022. Study on the effect of *Pogostemon Cablin Benth* on skin aging based on network pharmacology. Curr Comput-aid Drug. 18(6):459-468.
17. Hoffmann J, Gendrisch F, Schempp CM, Wölfle U. 2020. New herbal biomedicines for the topical treatment of dermatological disorders. Biomedicines. 8(2):27.
18. Wu N, Yuan T, Yin Z, Yuan X, Sun J, Wu Z, *et al*. 2022. Network pharmacology and molecular docking study of the Chinese Miao Medicine Sidaxue in the treatment of rheumatoid arthritis. Drug Des Dev Ther. 16:435-466.
19. Jiao X, Jin X, Ma Y, Yang Y, Li J, Liang L, *et al*. 2021. A comprehensive application: Molecular docking and network pharmacology for the prediction of bioactive constituents and elucidation of mechanisms of action in component-based Chinese medicine. Comput Biol Chem. 90:107402.
20. Shi SH, Cai YP, Cai XJ, Zheng XY, Cao DS, Ye FQ, *et al*. 2014. A network pharmacology approach to understanding the mechanisms of action of traditional medicine: Bushenhuoxue

formula for treatment of chronic kidney disease. PLoS ONE. 9(3):e89123.

21. Li X, Miao F, Xin R, Tai Z, Pan H, Huang H, *et al*. 2023. Combining network pharmacology, molecular docking, molecular dynamics simulation, and experimental verification to examine the efficacy and immunoregulation mechanism of FHB granules on vitiligo. Front Immunol. 14:1194823.
22. Chou HJ, Kuo JT, Lin ES. 2009. Comparative antioxidant properties of water extracts from different parts of beefsteak plant (*Perilla frutescens*). J Food Drug Anal. 17(6):489-496.
23. Pusadee T, Prom-u-thai C, Yimyam N, Jamjod S, Rerkasem B. 2017. Phenotypic and genetic diversity of local *Perilla* (*Perilla frutescens* (L.) Britt.) from northern Thailand. Econ Bot. 71(2):175-187.
24. Asif M. 2011. Health effects of omega-3,6,9 fatty acids: *Perilla frutescens* is a good example of plant oils. Orient Pharm Exp Med. 11(1):51-59.
25. Longvah T, Deosthale YG, Uday Kumar P. 2000. Nutritional and short term toxicological evaluation of *Perilla* seed oil. Food Chem. 70(1):13-16.
26. Thomas SS, Kim M, Lee SJ, Cha YS. 2018. Antiobesity effects of purple *Perilla* (*Perilla frutescens* var. acuta) on adipocyte differentiation and mice fed a high-fat diet. J Food Sci. 83(9):2384-2393.
27. Lee HA, Han JS. 2012. Anti-inflammatory effect of *Perilla frutescens* (L.) Britton var. frutescens extract in LPS-stimulated RAW 264.7 macrophages. PNF. 17(2):109-115.
28. Ueda H, Yamazaki C, Yamazaki M. 2002. Luteolin as an anti-inflammatory and anti-allergic constituent of *Perilla frutescens*. Biol Pharm bull. 25(9):1197-1202.
29. Khanaree C, Punfa W, Tantipaiboonwong P, Suttajit M, Chewonarin T, Pangjit K, *et al*. 2021. The attenuation of TNF-α-mediated Inflammatory responses in human lung adenocarcinoma cell line by *Perilla* seed and seed meal extract. CMU J Nat Sci. 20(4):1-15.
30. Thiboutot D. 2004. Regulation of human sebaceous glands. J Invest Dermatol. 123(1):1-12.
31. Cheng L, Guo J, Lu Y. 2023. Inhibition of lipogenesis and sebum secretion for *Lotus corniculatus* seed extract *in vitro* and *in vivo*. Int J Cosmetic Sci. 45(1):62-72.
32. Fan Y, Cao X, Zhang M, Wei S, Zhu Y, Ouyang H, *et al*. 2022. Quantitative comparison and chemical profile analysis of different medicinal parts of *Perilla frutescens* (L.) Britt. from different varieties and harvest periods. J Agric Food Chem. 70(28):8838-8853.
33. Lee YH, Kim B, Kim S, Kim MS, Kim H, Hwang SR, *et al*. 2017. Characterization of metabolite profiles from the leaves of green *perilla* (*Perilla frutescens*) by ultra high performance liquid chromatography coupled with electrospray ionization quadrupole time-of-flight mass spectrometry and screening for their antioxid. J Food Drug Anal. 25(4):776-788.
34. Deguchi Y, Ito M. 2020. Caffeic acid and rosmarinic acid contents in genus *Perilla*. J Nat Med-Tokyo. 74(4):834-839.
35. Liu J, Wan Y, Zhao Z, Chen H. 2013. Determination of the content of rosmarinic acid by HPLC and analytical comparison of volatile constituents by GC-MS in different parts of *Perilla frutescens* (L.) Britt. Chem Cent J. 7(1):1-11.
36. Deguchi Y, Ito M. 2020. Rosmarinic acid in *Perilla frutescens* and *perilla* herb analyzed by HPLC. J Nat Med-tokyo. 74(2):341-352.
37. Wang P, Jin B, Lian C, Guo K, Ma C. 2022. Comparative analysis of polycyclic aromatic hydrocarbons and halogenated polycyclic aromatic hydrocarbons in different parts of *Perilla frutescens* (L.) Britt. Molecules. 27(10):3133.
38. Saeidi S, Chamaie-Nejad F, Ebrahimi A, Najafi F, Rahimi Z, Vaisi-Raygani A, *et al*. 2018. PPAR-γ Pro12Ala and C161T polymorphisms in patients with acne vulgaris: Contribution to lipid and lipoprotein profile. Adv Med. 63(1):147-151.
39. Ekiz O, Balta I, Unlu E, Bulbul Sen B, Rifaioğlu EN, Dogramaci AC. 2015. Assessment of thyroid function and lipid profile in patients with postadolescent acne in a Mediterranean population from Turkey. Int J Dermatol. 54(12):1376-1381.
40. Caron A, Richard D, Laplante M. 2015. The roles of mTOR complexes in lipid metabolism. Annu Rev Nutr. 35(1):321-348.
41. Bennett NC, Gardiner RA, Hooper JD, Johnson DW, Gobe GC. 2010. Molecular cell biology of androgen receptor signaling. Int J Biochem Cell B. 42(6):813-827.
42. Singh R, Artaza JN, Taylor WE, Braga M, Yuan X, Gonzalez-Cadavid NF, *et al*. 2006. Testosterone inhibits adipogenic differentiation in 3T3-L1 cells: Nuclear translocation of androgen receptor complex with β-catenin and T-cell factor 4 may bypass canonical Wnt signaling to down-regulate adipogenic transcription factors. Endocrinology. 147(1):141-154.
43. Tao Q, Du J, Li X, Zeng J, Tan B, Xu J, *et al*. 2020. Network pharmacology and molecular docking analysis on molecular targets and mechanisms of Huashi Baidu formula in the treatment of COVID-19. Drug Dev Ind Pharm. 46(8):1345–1353.
44. Astragali R. 2023. Predicting the anti-inflammatory mechanism of *Radix Astragali* using network pharmacology and molecular docking. Medicine (Baltimore). 102(35):e34945.